Proton-glass dielectric behavior and phase diagram of $Cs_{1-x}(NH_4)_xH_2AsO_4$

T. K. Song, S. E. Moon, K. H. Noh, and S.-I. Kwun
Department of Physics, Seoul National University, Seoul 151-742, Korea

H.-K. Shin* and J.-J. Kim
Physics Department, Korea Advanced Institute of Science and Technology, 373-1 Kusung-dong, Yusung-ku, Taejon 305-701, Korea

(Received 11 March 1994; revised manuscript received 24 May 1994)

The complex dielectric constants of mixed $Cs_{0.80}(NH_4)_{0.20}H_2AsO_4$ single crystals have been measured in the temperature range from 13 to 200 K and the frequency range from 4.4 to 624 kHz along the a and c axes. Proton-glass behavior is first observed in the low-temperature region. The asymmetric concentration-temperature (x-T) phase diagram is obtained by measuring the complex dielectric constants of mixed $Cs_{1-x}(NH_4)_xH_2AsO_4$ microcrystalline powder pellets for the full range of mixing concentration x from 0 to 1. Proton-glass behavior develops in the concentration range of $0.12 < x < 0.51$. Coexistence of the proton-glass phase with the respective long-range ordering is observed in the two phase boundary regions.

I. INTRODUCTION

The proton-glass state was first observed in mixed crystals of ferroelectric RbH_2PO_4 (RDP) and antiferroelectric $NH_4H_2PO_4$ (ADP) by Courtens and has since received much attention.[1] Proton (deuteron) glass behavior has been also observed in the arsenate or deuterated analogs, such as $Rb_{1-x}(NH_4)_xH_2AsO_4$ (RADA), $Rb_{1-x}(ND_4)_xD_2PO_4$ (D-RADP), and $Rb_{1-x}(ND_4)_xD_2AsO_4$ (D-RADA) in intermediate mixing concentrations.[2–5] Because the lattice constants of RDP are similar to those of ADP, RDP is easily mixed with ADP. Recently proton-glass states were also observed in the potassium systems $K_{1-x}(NH_4)_xH_2PO_4$ (KADP) and $K_{1-x}(NH_4)_xH_2AsO_4$ (KADA),[6,7] although the crystal growth of KADP is more difficult than $Rb_{1-x}(NH_4)_xH_2PO_4$ (RADP) due to the large lattice mismatches between KH_2PO_4 (KDP) and ADP or between KH_2AsO_4 (KDA) and $NH_4H_2AsO_4$ (ADA). However, powder pellet systems are shown to have proton-glass behavior very similar to those of single crystals as confirmed by dielectric measurement[8] and Raman study.[9]

In this work we have studied the cesium systems $Cs_{0.80}(NH_4)_{0.20}H_2AsO_4$ single crystals and $Cs_{1-x}(NH_4)_xH_2AsO_4$ (CADA) powder pellets. CsH_2AsO_4 (CDA, T_C=143 K) and ADA (T_N=217 K) have tetragonal structure in the paraelectric phase and are transformed to the orthorhombic structure below the respective transition temperatures.[10]

II. EXPERIMENTAL DETAILS

A pure ADA solution was obtained by reacting ammonium carbonate with an arsenic acid solution. CDA solutions were made by reacting CsOH solution with an arsenic acid solution. Each powder of ADA or CDA was obtained by drying the saturated solution. By weighing and dissolving the parent powders in molar ratios, aqueous mixture solutions were prepared. Single crystals were grown by slow evaporation from the saturated solution at 35±0.2 °C. The concentration x was determined to be 0.20 by atomic absorption analysis. The sample size of the a cut crystal was $5 \times 4 \times 0.31$ mm^3, and that of the c cut crystal was $4.5 \times 4 \times 0.35$ mm^3.

For making powder samples, the solutions were stirred for several hours for sufficient mixing, and CADA powder was obtained by drying the solutions slowly. The crystal structure of the powder microcrystals was determined by x-ray diffraction to be tetragonal with its lattice constants between those of CDA and ADA. The powder was pressed to form pellets with thickness of 1 mm and diameter 10 mm. The mixing concentrations of the pellet samples were analyzed by the titration method. Electrodes were formed on each face with a diameter of 7 mm by applying silver paint.

The complex dielectric constants $\epsilon'(\omega,T)$ and $\epsilon''(\omega,T)$ were measured by a low frequency LCR meter (HP4192A) in the frequency range from 4.4 to 624 kHz for the single crystals and from 316 Hz to 316 kHz for the pellet samples. A multifrequency LCR meter (HP4275A) was also used with a frequency range from 10 to 400 kHz. A closed cycle helium refrigerator (APD Ltd.) was used to cool down the samples to 13 K. The cooling rate was controlled to be about 0.5 K/min for the single crystal and 1.0 K/min for the pellet sample measurements.

III. RESULTS AND DISCUSSION

Figure 1(a) shows the temperature dependence of the real dielectric constants of a CADA (x=0.20) single crys-

tal along the a axis. The solid line shows the Curie-Weiss fit, which is well obeyed down to the freezing onset temperature T_f = 108 K at 8 kHz. The Curie-Weiss temperature T_{CW} the extrapolated temperature at which the inverse real dielectric constant would vanish is deduced to be −89 K and the Curie constant C to be 13 646 K. The freezing onset temperature T_f of the CADA (x=0.20) single crystal is higher than the 70 K T_f of $Rb_{0.65}(NH_4)_{0.35}H_2AsO_4$ [RADA (x=0.35)] at 30 kHz and the 85 K T_f of $K_{0.60}(NH_4)_{0.40}H_2AsO_4$ [KADA (x=0.40)] at 10 kHz. For RADA (x=0.35) and KADA (x=0.40) the Curie-Weiss temperatures T_{CW}'s are reported to be −69 K and −32 K, and the Curie constants C to be 19 320 K and 20 380 K, respectively.[2,7] Figures 1(b) and 1(c) show the dielectric dispersions in the proton-glass regime. The glass transition temperature T_g at which ϵ' starts to decrease and ϵ'' to increase, as defined in the previous work, is about 55 K at 32 kHz, which is higher than 38 K of RADA(x=0.35) and 40 K of KADA(x=0.40) at 30 kHz.[2,7] This result seems related to the fact that the ferroelectric transition temperature 143 K of CDA is much higher than 110 K of RDA or 97 K of KDA.[10]

Figure 2(a) shows the temperature dependence of the real dielectric constant of a CADA (x=0.20) single crystal along the c axis, where we find T_f to be 94 K, T_{CW} to be −36 K, and C to be 2950 K at 8 kHz. Figures 2(b) and 2(c) show dielectric dispersion along the c axis. Because of the piezoelectric resonance interference, the frequency range of our reliable measurements is narrow for this measurement.

Figure 3(a) shows the temperature dependence of the real dielectric constants of CADA (x=0.22) powder pellets. The overall behaviors are very similar to those of the CADA (x=0.20) single crystal along the a axis. The microcrystalline grains have an average size of a few μm in diameter as examined under an optical microscope. Figures 3(b) and 3(c) show the proton-glass dielectric dispersion of the CADA (x=0.22) powder pellet. The complex dielectric constants in a wide frequency range are measured with high resolution.

As a test sample, a pellet of average composition x = 0.22 was made by mechanical mixing of pure ADA and CDA powders. This powder seems from x-ray diffraction

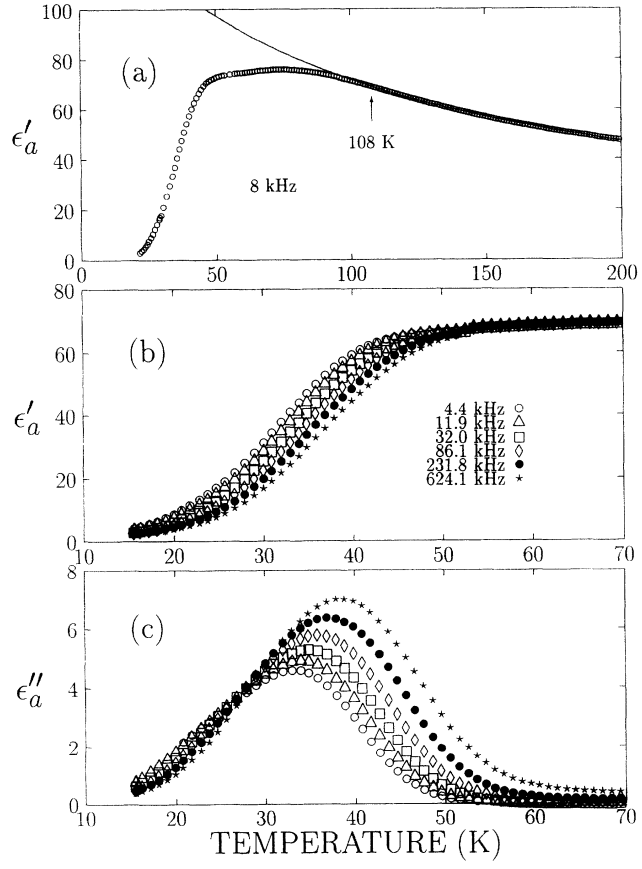

FIG. 1. (a) The temperature dependence of the real dielectric constant ϵ'_a in a CADA (x=0.20) single crystal along the a axis. The solid line shows the Curie-Weiss fit. (b) The real $\epsilon'_a(\omega,T)$ and (c) imaginary $\epsilon''_a(\omega,T)$ dielectric dispersions in the proton-glass regime.

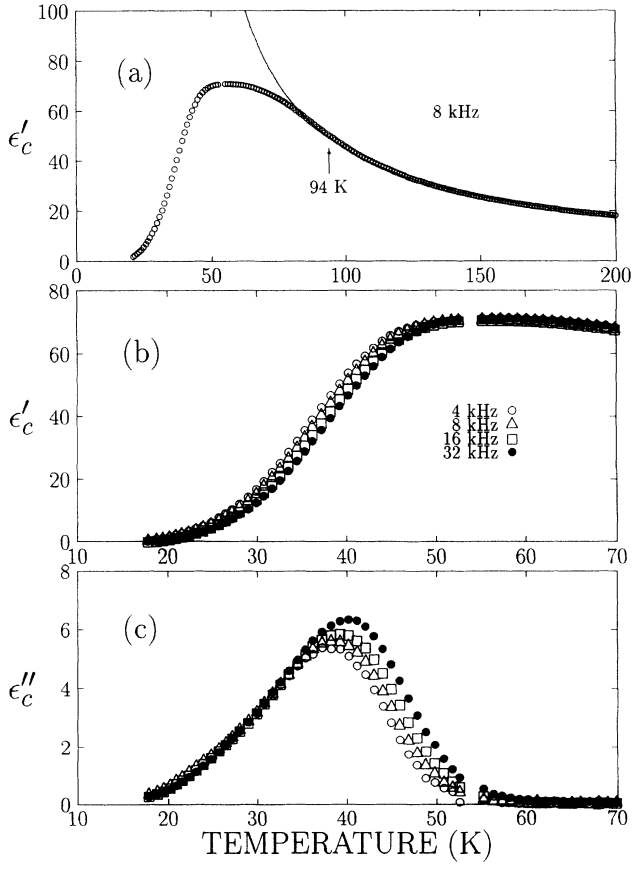

FIG. 2. (a) The temperature dependence of the real dielectric constant ϵ'_c in a CADA (x=0.20) single crystal along the c axis. The solid line shows the Curie-Weiss fit. (b) The real $\epsilon'_c(\omega,T)$ and (c) imaginary $\epsilon''_c(\omega,T)$ dielectric dispersion in the proton-glass regime.

to consist of ADA and CDA grains. An antiferroelectric transition cusp and a ferroelectric transition peak were observed separately in the dielectric measurement at the respective transition temperatures without the proton-glass behavior for this ADA/CDA powder mixture.

The Cole-Cole plot for the $x = 0.22$ powder pellet sample is shown in Fig. 4. As the temperature decreases below T_g there appears an increasingly broader distribution of relaxation times. Similar results are reported for D-RADA (x=0.25), RADA (x=0.10), and D-RADA (x=0.10).[11,12] The dielectric relaxation in the low-temperature region (30–40 K) was found to satisfy the Vogel-Fulcher equation[13,14]

$$\nu_c = \nu_0 \exp[-E_C/(T - T_0)],$$

where T_0 is the Vogel-Fulcher temperature, E_C the activation barrier height, ν_0 the attempt frequency, and ν_c the observed cutoff frequency. The best fit to this equation was obtained as shown in Fig. 5 for the following values of the parameters: $T_0 = 10.1$ K, E_C=449 K, and $\nu_0 = 3.15 \times 10^{12}$ Hz.

Figure 6(a) shows the temperature dependence of the real dielectric constants for pellet samples of $x = 0.0$, 0.035, and 0.12. For $x = 0.0$ corresponding to pure CDA,

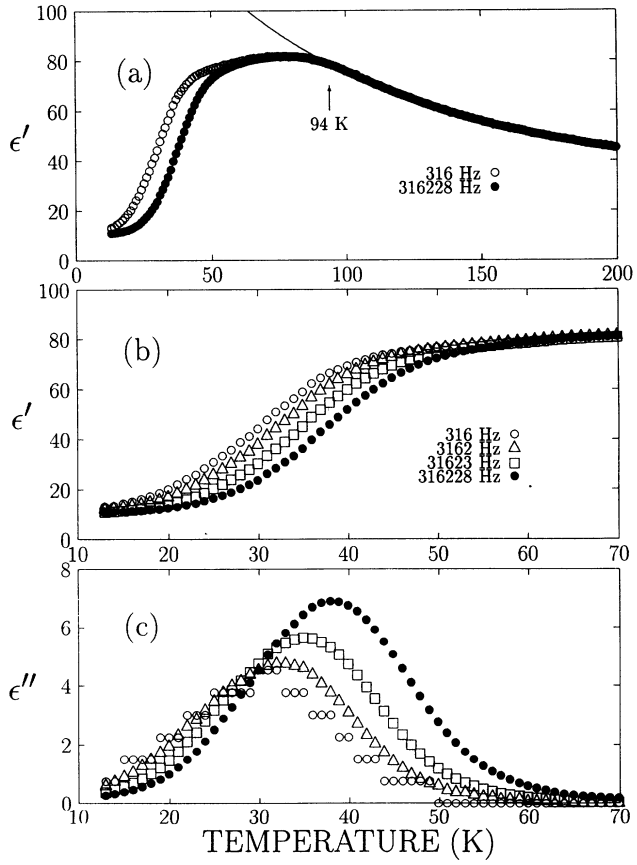

FIG. 3. (a) The temperature dependence of the real dielectric constant ϵ' in a CADA (x=0.22) pellet sample. The solid line shows the Curie-Weiss fit. (b) The real $\epsilon'(\omega, T)$ and (c) imaginary $\epsilon''(\omega, T)$ dielectric dispersions of a CADA (x=0.22) pellet sample in the proton-glass regime.

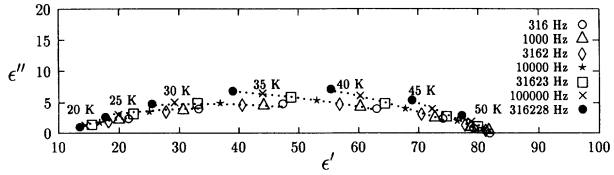

FIG. 4. Cole-Cole plot for a CADA (x=0.22) powder sample in the proton-glass regime.

a typical ferroelectric transition at 143 K and domain wall freezing behavior at about 95 K were observed. For $x = 0.035$ the ferroelectric transition temperature is decreased to 141 K as expected from the impurity effect. As ammonium concentration is increased to $x = 0.12$, the ferroelectric transition is rounded with the transition temperature falling down to about 114 K, and proton-glass behavior starts to be observed. This behavior may be like the coexistence of the proton-glass phase and ferroelectric long-range ordering as reported in RADA system.[15,16] Although the possibility of inhomogeneous concentration in the pellet sample cannot be ruled out, a single phase crystalline structure was confirmed through x-ray diffraction.

Figure 6(b) shows the temperature dependence of the real dielectric constants for samples of $x = 0.22$, 0.33, and 0.43. Proton-glass behavior was observed for $x = 0.22$ and 0.33. For $x = 0.43$ a very diffuse antiferroelectric transition appeared around 120 K together with proton-glass behavior at lower temperature. Figure 6(c) shows the temperature dependence of the real dielectric constants for $x = 0.51$, 0.75, and 1.0. For $x = 0.51$ a reduced and rounded antiferroelectric phase transition cusp around 157 K was observed along with proton-glass behavior at lower temperature. An antiferroelectric phase transition was revealed around 191 K for $x = 0.75$. The

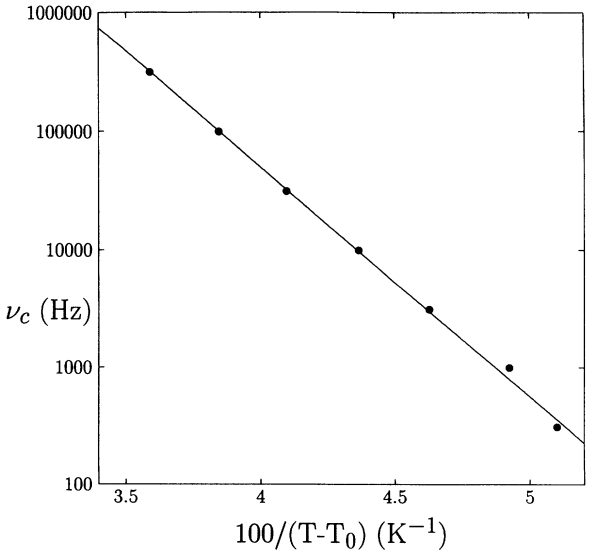

FIG. 5. The Vogel-Fulcher dependence for a CADA (x=0.22) pellet sample in the proton-glass regime.

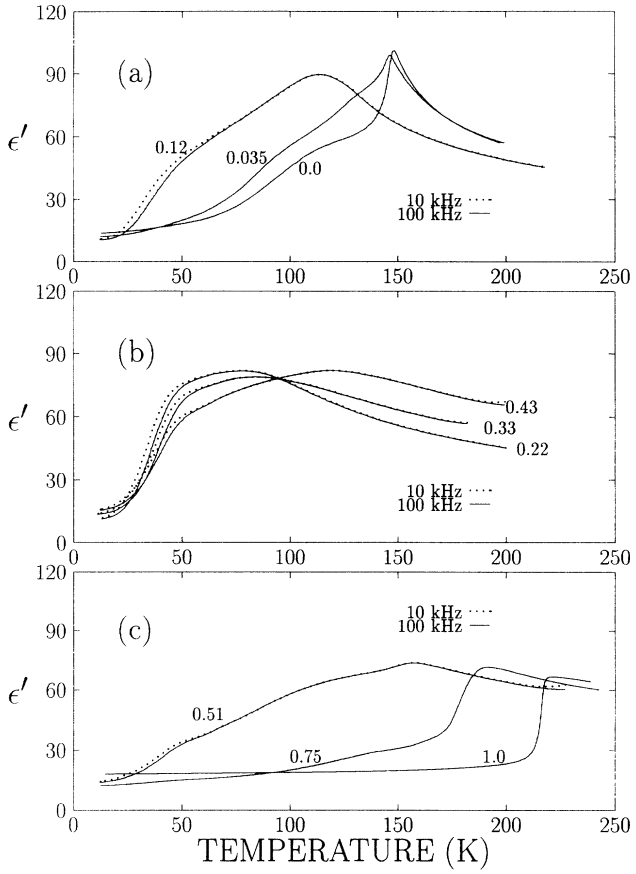

FIG. 6. The temperature dependence of the real dielectric constant ϵ' of CADA pellets for (a) the ferroelectric region, $x = 0.0$, 0.035, and 0.12, (b) proton-glass region, $x = 0.22$, 0.33, and 0.43, and (c) the antiferroelectric region, $x = 0.51$, 0.75, and 1.0.

$x = 1.0$ sample, pure ADA, depicted a sharp antiferroelectric transition at 217 K.

Summarizing all the above results, an asymmetric x-T phase diagram of CADA is obtained as shown in Fig. 7. In the figure, the ferroelectric transition temperature T_C and the antiferroelectric transition temperature T_N are determined to be the temperature at which the real dielectric constant ϵ' has its maximum value. The freezing temperature T_f is the temperature where real dielectric constant ϵ' starts to deviate from the Curie-Weiss law at 10 kHz, and the glass transition temperature T_g depends on the frequency of measurement, and is defined at 10 kHz for this diagram.

For the RADP system, the ratio of the antiferroelectric transition temperature to the ferroelectric phase transition temperature, T_N/T_C, of the two constituent pure crystals is 1.01, and the x-T phase diagram is symmetric with the proton-glass behavior observed in the wide concentration range from $x = 0.22$ to 0.75.[17] For the

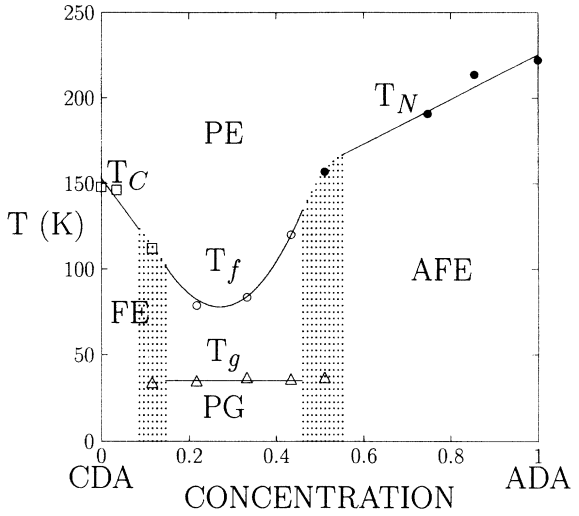

FIG. 7. The concentration-temperature (x-T) phase diagram of the CADA system: FE for ferroelectric, PE for paraelectric, AFE for antiferroelectric, PG for proton glass, T_C for ferroelectric transition temperature (empty square), T_N for antiferroelectric transition temperature (filled circle), T_f for freezing temperature (empty circle), and T_g for glass transition temperature (empty triangle), respectively. Dotted regions represent a possible two-phase coexistence.

RADA system, the ratio is 1.96, and an asymmetric x-T diagram has been obtained with the proton-glass behavior appearing in the mixing concentration from $x = 0.18$ to 0.45.[3,16] Coexistence of proton (deuteron)-glass and long-range ferroelectric ordering has been observed near the phase boundary between the ferroelectric and the proton-glass phase in RADA.[15,16] These phenomena have not been reported in the RADP system, although such coexistence was recently reported in deuterated D-RADP based on NMR measurements.[18]

In this CADA system, the ratio T_N/T_C is 1.52. An asymmetric x-T phase diagram with the proton-glass concentration x from 0.12 to 0.51 is obtained. Phase coexistence of proton-glass and ferroelectric ordering or proton glass and antiferroelectric ordering seems to occur for the concentrations in the phase boundary regions between the proton glass and the respective long-range ordering.

ACKNOWLEDGMENTS

The authors thank Professor J.-G. Yoon of Suwon University for helpful discussions. They also thank Dr. Y. H. Kim of Korea Institute of Science and Technology (KIST) for analyzing the chemical concentrations of the powder pellet samples. This work was supported by the Seoul National University (S.N.U.) Daewoo Research Fund.

* Present address: Physics Department, Daejean University, Pocheon, Kyunggi-do, Korea.

[1] E. Courtens, J. Phys. (Paris) Lett. **43**, L199 (1982).
[2] Z. Trybula, V. H. Schmidt, J. E. Drumheller, D. He, and Z. Li, Phys. Rev. B **40**, 5289 (1989).
[3] S. Kim and S.-I. Kwun, Phys. Rev. B **42**, 638 (1990).
[4] V. H. Schmidt, S. Waplak, S. Hutton, and P. Schnackenberg, Phys. Rev. B **30**, 2795 (1984).

[5] Z. Trybula, J. Stankowski, L. Szczepanska, R. Blinc, A. Weiss, and N. S. Dalal, Physica B **153**, 143 (1988).
[6] Y. Ono, T. Hikita, and T. Ikeda, Ferroelectrics **79**, 327 (1988).
[7] Z. Trybula, V. H. Schmidt, and J. E. Drumheller, Phys. Rev. B **42**, 6733 (1990).
[8] O. J. Kwon and J.-J. Kim, Phys. Rev. B **48**, 6639 (1993).
[9] J.-J. Kim and W. F. Sherman, Phys. Rev. B **36**, 5651 (1987).
[10] *Ferro- and Antiferroelectric Substances*, edited by K.-H. Hellwege, Landolt-Börnstein, New Series, Group III, Vols. 3 and 9 (Springer-Verlag, Berlin, 1969 and 1975).
[11] Z. Kutnjak, A. Levstik, C. Filipic, R. Pirc, B. Tadic, R. Blinc, H. Kabelka, A. Fuith, and H. Warhanek, J. Phys. Condens. Matter **3**, 91 (1991); Z. Kutnjak, C. Filipic, A. Levstik, and R. Pirc, Phys. Rev. Lett. **70**, 4015 (1993).
[12] F. L. Howell, N. J. Pinto, and V. H. Schmidt, Phys. Rev. B **46**, 13762 (1992).
[13] E. Courtens, Phys. Rev. Lett. **52**, 69 (1984).
[14] Z. Trybula, J. Stankowski, and S. Los, Physica B **191**, 312 (1993).
[15] J. Eom, J.-G. Yoon, and S.-I. Kwun, Phys. Rev. B **44**, 2826 (1991).
[16] Z. Trybula, V. H. Schmidt, and J. E. Drumheller, Phys. Rev. B **43**, 1287 (1991).
[17] E. Courtens, Jpn. J. Appl. Phys. **24**, Suppl. 24-2, 70 (1985).
[18] N. Korner, C. Pfammatter, and R. Kind, Phys. Rev. Lett. **70**, 1283 (1993).